Supporting information for

Sustainable and Energy-Saving Hydrogen Production via Binder-free and In-situ Electrodeposited Ni-Mn-S Nanowires on Ni-Cu 3-D Substrate

Ghasem Barati Darband[a*], Danial Iravani[b], Meiling Zhang[c], Meysam Maleki[d], Shanrui Huang[c], Reza Andaveh[e], Seyyed Mehdi Khoshfetrat[f], Jinyang Li[c,g*]

a- Materials and Metallurgical Engineering Department, Faculty of Engineering, Ferdowsi University of Mashhad, Mashhad 91775-1111, Iran
b- Chemical Engineering Department, Faculty of Engineering, Ferdowsi University of Mashhad, Mashhad, Iran
c- School of Chemistry, Key Laboratory of Advanced Technologies of Materials (Ministry of Education), Southwest Jiaotong University, Chengdu 610031, China
d- Department of Chemical and Materials Engineering, Concordia University, Montreal, Quebec H4B 1R6, Canada
e- Department of Mechanical and Materials Engineering, University of Western Ontario, London, Ontario, N6A 5B9 Canada
f- Department of Chemistry, Faculty of Basic Science, Ayatollah Boroujerdi University, Borujerd, Iran
g- Yibin Institute of Southwest Jiaotong University, Yibin 644000, China

* Corresponding authors
Ghasem Barati Darband: baratidarband@um.ac.ir
Jinyang Li: jinyang.li@swjtu.edu.cn.

Table S1: Composition of electrolyte for deposition of Ni-Cu nano-micro dendrites

Materials	**Concentration (M)**
$NiSO_4.6\ H_2O$	0.5
$CuSO_4.5\ H_2O$	0.01
HCl	1
H_2SO_4	1.5

Table S2: Composition of electrolyte for deposition of Ni-Cu nano-micro dendrites

Materials	**Concentration**
$NiCl_2.6\ H_2O$	5 mM
$MnCl_2.4\ H_2O$	5 mM
H_2NCSNH_2	0.075 M

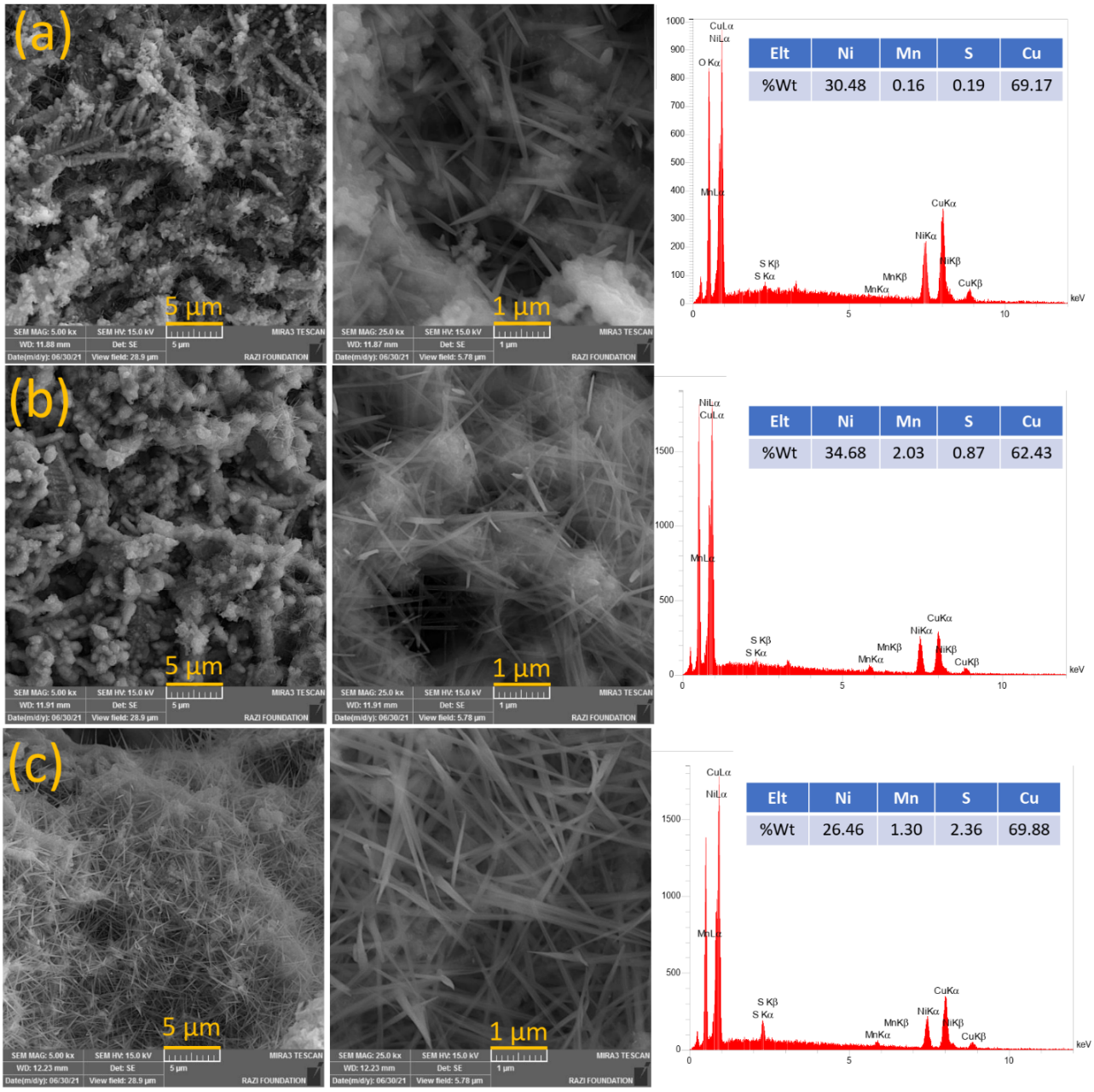

Fig. S1. FESEM and EDX images of Ni-Mn-S/Ni-Cu samples fabricated at different coating cycles: (a) 3, (b) 5, and (c) 20 cycles.

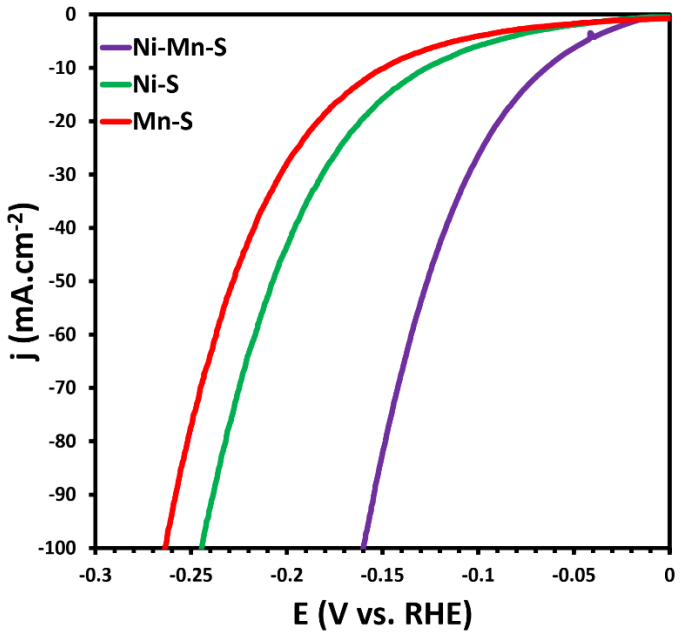

Figure S2: LSV curves of different electrodes.

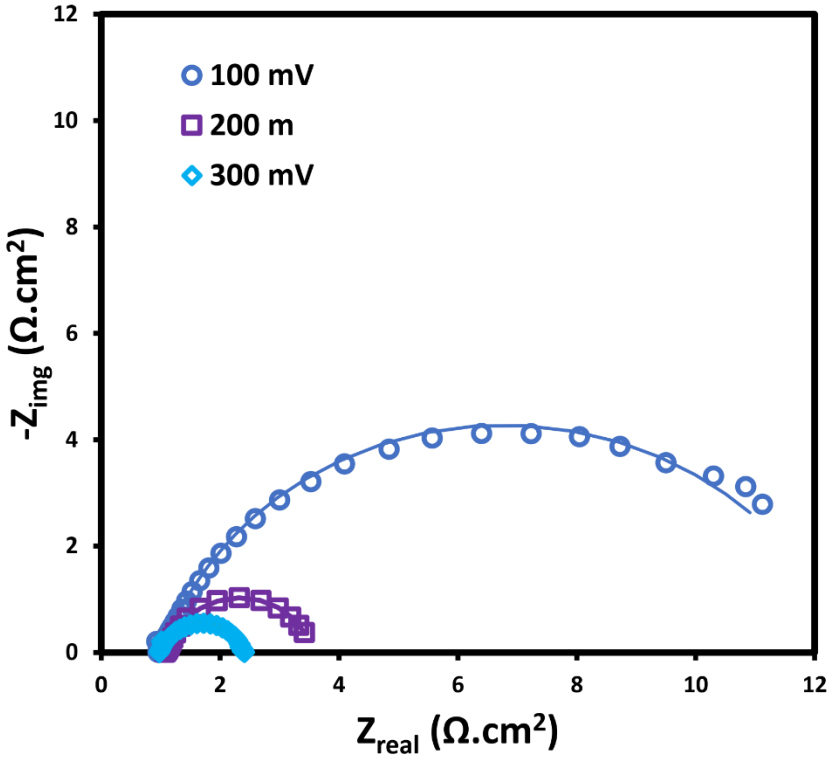

Figure S3: Nyquist curves at different overpotentials of optimized electrode.

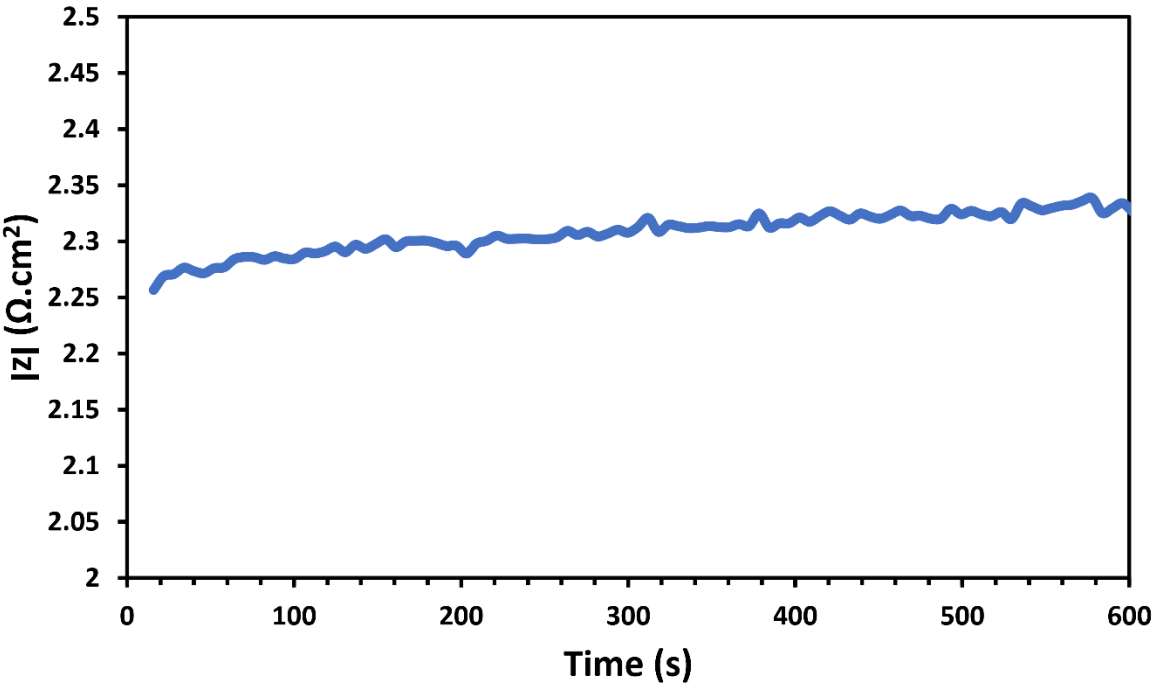

Figure S4: dynamic specific resistance at fixed frequency.

Table S3: Comparison of HER properties for different electrocatalysts in 1.0 M KOH solution.

Catalyst	Substrate	Tafel slope (mV dec−1)	Overpotential (mV)	Stability	Ref.
Mo-NiSx/NF	NF	88.0	η10 = 155	50 h at 10 mA cm−2	[1]
V-Ni3N	NF	28.7	η10 = 15	24 h at 10 mA cm−2	[2]
NiCu/NiMn(OH)2	NF	31.0	η10 = 17	50 h at 10 mA cm−2	[3]
S-Ni@Ni(OH)2/NF	NF	74.0	η10 = 50	15 h at 80 mV	[4]
Ni-Co-Fe-P	NF	67.0	η10 = 64	100 h at 100 mA cm−2	[5]
MnCo/NiSe	NF	45.1	η10 = 22	200 h at 500 mA cm−2	[6]
NiMo@Ni(OH)2MoOx	GR	115.0	η100 = 160	24 h at 100 mA cm−2	[7]
NiCoSeP	NF	59.0	η10 = 52	15 h at 500 mA cm−2	[8]
P-doped NiSe	NF	117.0	η10 = 90	100 h at 100 mA cm−2	[9]
Nanoporous Ni-Se	GR	126.0	η10 = 100	12 h at 100 mA cm−2	[10]
Ni-P/Ni(OH)2 NTs	NF	58.0	η10 = 55	30 h at 10 mA cm−2	[11]
NiMn1.5PO4/NF	NF	43.0	η10 = 72	50 h at 10 mA cm−2	[12]
O-NiCoP/Ni2P	NF	68.8	η10 = 58	24 h at 10 mA cm−2	[13]
Ni-Mo-O/Ni4Mo@NC	CP	99.0	η10 = 61	15 h at 10 mA cm−2	[14]
V-doped NiSe/Ni3Se2	NF	70.0	η100 = 175	11 h at 100 mA cm−2	[15]
NiSe2-Ni2P/NF	NF	68.0	η10 = 102	25 h at 150 mV	[16]
Ni-Mn-S/Ni-Cu/10	NF	81.0	η10 =64	24 h at 100 mA cm−2	This work

Table S4: Comparison of UOR properties for different electrocatalysts.

Catalyst	Substrate	Solution	Tafel slope (mV dec^{-1})	Potential vs. RHE (V)	Stability	Ref.
$Co_2P/NiMoO_4/NF$	NF	1.0 M KOH + 0.50 M urea	75.0	E_{10} = 1.34	50 h at 1.37 V	[17]
Ni_3N/Mo_2N	NF	1.0 M KOH + 0.33 M urea	34.7	E_{100} = 1.36	40 h at 120 mA cm^{-2}	[18]
Ni-Mn-Se	NF	1.0 M KOH + 0.33 M urea	58.2	E_{100} = 1.44	50 h at 200 mA cm^{-2}	[19]
$W\text{-}NiS_2/MoO_2$@CC	CC	1.0 M KOH + 0.33 M urea	24.1	E_{10} = 1.30	24 h at 1.40 V	[20]
$NF/PPy_{700}\text{-}Ni_3S_2\text{-}8\text{-}Ar$	NF	1.0 M KOH + 0.33 M urea	20.0	E_{20} = 1.35	12 h at 20 mA cm^{-2}	[21]
$FeNi_3\text{-}MoO_2/NF$	NF	1.0 M KOH + 0.50 M urea	30.1	E_{10} = 1.29	120 h at 500 mA cm^{-2}	[22]
Mo-doped Ni_3S_2	NF	1.0 M KOH + 0.30 M urea	28.1	E_{10} = 1.33	120 h at 10 mA cm^{-2}	[23]
$Ni_9S_8/CuS/Cu_2O$	NF	1.0 M KOH + 0.33 M urea	64.0	E_{10} = 1.36	20 h at 1.36 V	[24]
$NiCo_2S_4$/CC	CC	1.0 M KOH + 0.33 M urea	172.0	E_{50} = 1.43	10 h at 1.37 V	[25]
NiCo-BDC/Ni-S	NF	1.0 M KOH + 0.33 M urea	58.2	E_{10} = 1.31	52 h at 10 mA cm^{-2}	[26]
$P\text{-}CoS_x(OH)_yNN/Ti$	TM	1.0 M KOH + 0.50 M urea	104.0	E_{10} = 1.30	40 h at 1.48 V	[27]
$Ni(OH)_2$@NF	NF	1.0 M KOH + 0.30 M urea	24.4	E_{10} = 1.35	40 h at 10 mA cm^{-2}	[28]
$Ni_4N/Cu_3N/CF$	CF	1.0 M KOH + 0.50 M urea	55.7	E_{10} = 1.34	10 h at 100 mA cm^{-2}	[29]
Ni_3N/NF	NF	1.0 M KOH + 0.50 M urea	41.0	E_{10} = 1.34	36 h at 1.37 V	[30]
NiFeCo LDH/NF	NF	1.0 M KOH + 0.33 M urea	31.0	E_{10} = 1.35	50 h at 10 mA cm^{-2}	[31]
$NiFe(OH)_2$-SD/NF	NF	1.0 M KOH + 0.50 M urea	41.0	E_{10} = 1.32	24 h at 10 mA cm^{-2}	[32]
Ni-Mn-S/Ni-Cu/10	NF	1.0 M KOH + 0.33 M urea	87.0	E_{10} = 1.247	24 h at 100 mA cm^{-2}	This work

Table S5: Comparison of overall urea electrolysis properties for different electrocatalysts.

Catalyst	Substrate	Solution	Cell potential vs. RHE (V)	Stability	Ref.
Ni_3N/Mo_2N	NF	1.0 M KOH + 0.33 M urea	ΔE_{10} = 1.36	50 h at 10 mA cm^{-2}	[18]
Ni-Mn-Se	NF	1.0 M KOH + 0.33 M urea	ΔE_{100} = 1.62	50 h at 50 mA cm^{-2}	[19]
W-NiS_2/MoO_2@CC	CC	1.0 M KOH + 0.33 M urea	ΔE_{10} = 1.37	24 h at 1.40 V	[20]
NF/PPy_{700}-Ni_3S_2-8-Ar	NF	1.0 M KOH + 0.33 M urea	ΔE_{20} = 1.50	20 h at 1.60 V	[21]
$FeNi_3$-MoO_2/NF	NF	1.0 M KOH + 0.50 M urea	ΔE_{10} = 1.37	70 h at 100 mA cm^{-2}	[22]
Mo-doped Ni_3S_2	NF	1.0 M KOH + 0.30 M urea	ΔE_{10} = 1.45	120 h at 10 mA cm^{-2}	[23]
$Ni_9S_8/CuS/Cu_2O$	NF	1.0 M KOH + 0.33 M urea	ΔE_{10} = 1.47	20 h at 1.47 V	[24]
$NiCo_2S_4$/CC	CC	1.0 M KOH + 0.33 M urea	ΔE_{10} = 1.45	15 h at 1.51 V	[25]
NiCo-BDC/Ni-S	NF	1.0 M KOH + 0.33 M urea	ΔE_{10} = 1.46	50 h at 10 mA cm^{-2}	[26]
P-$CoS_x(OH)_y$NN/Ti	TM	1.0 M KOH + 0.50 M urea	ΔE_{10} = 1.30	40 h at 1.29 V	[27]
$Ni(OH)_2$@NF	NF	1.0 M KOH + 0.30 M urea	ΔE_{50} = 1.45	40 h at 20 mA cm^{-2}	[28]
Ni_4N/Cu_3N/CF	CF	1.0 M KOH + 0.50 M urea	ΔE_{10} = 1.48	10 h at 100 mA cm^{-2}	[29]
Ni_3N/NF	NF	1.0 M KOH + 0.50 M urea	ΔE_{100} = 1.42	20 h at 1.37 V	[30]
NiFeCo LDH/NF	NF	1.0 M KOH + 0.33 M urea	ΔE_{10} = 1.49	50 h at 10 mA cm^{-2}	[31]
Ni(OH)S/NF	NF	1.0 M KOH + 0.33 M urea	ΔE_{10} = 1.36	40 h at 20 mA cm^{-2}	[33]
Ni-Mn-S/Ni-Cu/10	NF	1.0 M KOH + 0.33 M urea	ΔE_{10} = 1.302	24 h at 50 mA cm^{-2}	This work

References

1. Zhang, Y., et al., *Magnetic field-enhanced water splitting enabled by bifunctional molybdenum-doped nickel sulfide on nickel foam.* Carbon Energy, 2023. **5**(10).
2. Ma, W., et al., *Formulating a heterolytic cleavage process of water on Ni3N nanosheets through single transition metal doping for ultra-efficient alkaline hydrogen evolution.* Inorganic Chemistry Frontiers, 2023. **10**(17): p. 5152-5160.
3. Li, Z., et al., *Boosting elementary steps kinetics towards energetic alkaline hydrogen evolution via dual sites on phase-separated Ni-Cu-Mn/hydroxide.* Chemical Engineering Journal, 2023. **451**: p. 138540.
4. Huang, W., et al., *Sulfur-Modified Nickel-Based Hybrid Nanosheet as a Robust Bifunctional Electrode for Hydrogen Generation via Formaldehyde Reforming.* ACS Applied Energy Materials, 2023. **6**(13): p. 7221-7229.
5. Darband, G.B., et al., *Electrodeposition of self-supported transition metal phosphides nanosheets as efficient hydrazine-assisted electrolytic hydrogen production catalyst.* International Journal of Hydrogen Energy, 2023. **48**(11): p. 4253-4263.
6. Andaveh, R., et al., *Boosting the electrocatalytic activity of NiSe by introducing MnCo as an efficient heterostructured electrocatalyst for large-current-density alkaline seawater splitting.* Applied Catalysis B: Environmental, 2023. **325**: p. 122355.
7. Zhao, M.-J., et al., *Indirect electrodeposition of a NiMo@Ni(OH)2MoOx composite catalyst for superior hydrogen production in acidic and alkaline electrolytes.* Renewable Energy, 2022. **191**: p. 370-379.
8. Maleki, M., et al., *Highly active and durable NiCoSeP nanostructured electrocatalyst for large-current-density hydrogen production.* ACS Applied Energy Materials, 2022. **5**(3): p. 2937-2948.
9. Maleki, M., et al., *Binder-free P-doped Ni-Se nanostructure electrode toward highly active and stable hydrogen production in wide pH range and seawater.* Journal of Electroanalytical Chemistry, 2022. **916**: p. 116379.
10. Arabi, M., A. Ghaffarinejad, and G.B. Darband, *Electrodeposition of nanoporous nickel selenide on graphite rod as a bifunctional electrocatalyst for hydrogen and oxygen evolution reactions.* Journal of Electroanalytical Chemistry, 2022. **907**: p. 116066.
11. Zhao, F., et al., *Amorphous/amorphous Ni-P/Ni(OH)2 heterostructure nanotubes for an efficient alkaline hydrogen evolution reaction.* Journal of Materials Chemistry A, 2021. **9**(16): p. 10169-10179.
12. Zhang, G., et al., *NiMn1.5PO4 thin layer supported on Ni foam as a highly efficient bifunctional electrocatalyst for overall water splitting.* Electrochimica Acta, 2021. **367**: p. 137567.
13. Wen, Y., et al., *O doping hierarchical NiCoP/Ni2P hybrid with modulated electron density for efficient alkaline hydrogen evolution reaction.* Applied Catalysis B: Environmental, 2021. **293**: p. 120196.
14. Jin, Z., et al., *Transition metal/metal oxide interface (Ni-Mo-O/Ni4Mo) stabilized on N-doped carbon paper for enhanced hydrogen evolution reaction in alkaline conditions.* Industrial & Engineering Chemistry Research, 2021. **60**(14): p. 5145-5150.

15. He, D., et al., *Tuning the morphologic and electronic structures of self-assembled NiSe/Ni3Se2 heterostructures with vanadium doping toward efficient electrocatalytic hydrogen production.* Applied Surface Science, 2021. **542**: p. 148598.
16. Wang, P., et al., *Coupling NiSe2-Ni2P heterostructure nanowrinkles for highly efficient overall water splitting.* Journal of catalysis, 2019. **377**: p. 600-608.
17. You, M., et al., *Novel trifunctional electrocatalyst of nickel foam supported Co2P/NiMoO4 heterostructures for overall water splitting and urea oxidation.* Journal of Colloid and Interface Science, 2023. **648**: p. 278-286.
18. Wang, T., et al., *Interfacial engineering of Ni3N/Mo2N heterojunctions for urea-assisted hydrogen evolution reaction.* ACS Catalysis, 2023. **13**(7): p. 4091-4100.
19. Maleki, M., et al., *Mn-incorporated nickel selenide: an ultra-active bifunctional electrocatalyst for hydrogen evolution and urea oxidation reactions.* Chemical Communications, 2022. **58**(21): p. 3545-3548.
20. Fereja, S.L., et al., *W-doping induced abundant active sites in a 3D NiS2/MoO2 heterostructure as an efficient electrocatalyst for urea oxidation and hydrogen evolution reaction.* Chemical Engineering Journal, 2022. **432**: p. 134274.
21. Zhang, Y., et al., *Coaxial Ni–S@N-doped carbon nanofibers derived hierarchical electrodes for efficient H2 production via urea electrolysis.* ACS Applied Materials & Interfaces, 2021. **13**(3): p. 3937-3948.
22. Xu, Q., et al., *Coupling interface constructions of FeNi3-MoO2 heterostructures for efficient urea oxidation and hydrogen evolution reaction.* ACS Applied Materials & Interfaces, 2021. **13**(14): p. 16355-16363.
23. Xu, H., et al., *A branch-like Mo-doped Ni3S2 nanoforest as a high-efficiency and durable catalyst for overall urea electrolysis.* Journal of Materials Chemistry A, 2021. **9**(6): p. 3418-3426.
24. Wei, D., W. Tang, and Y. Wang, *Hairy sphere-like Ni9S8/CuS/Cu2O composites grown on nickel foam as bifunctional electrocatalysts for hydrogen evolution and urea electrooxidation.* International Journal of Hydrogen Energy, 2021. **46**(40): p. 20950-20960.
25. Song, W., et al., *Construction of self-supporting, hierarchically structured caterpillar-like NiCo2S4 arrays as an efficient trifunctional electrocatalyst for water and urea electrolysis.* Nanoscale, 2021. **13**(3): p. 1680-1688.
26. Li, M., et al., *NiCo-BDC nanosheets coated with amorphous Ni-S thin film for high-efficiency oxygen evolution reaction and urea oxidation reaction.* FlatChem, 2021. **25**: p. 100222.
27. Jiang, Y., et al., *Porous and amorphous cobalt hydroxysulfide core-shell nanoneedles on Ti-mesh as a bifunctional electrocatalyst for energy-efficient hydrogen production via urea electrolysis.* Journal of Materials Chemistry A, 2021. **9**(9): p. 5664-5674.
28. Xia, L., et al., *In situ growth of porous ultrathin Ni(OH)2 nanostructures on nickel foam: an efficient and durable catalysts for urea electrolysis.* ACS Applied Energy Materials, 2020. **3**(3): p. 2996-3004.
29. Li, J., et al., *Boosting hydrogen production by electrooxidation of urea over 3D hierarchical Ni4N/Cu3N nanotube arrays.* ACS sustainable chemistry & engineering, 2019. **7**(15): p. 13278-13285.
30. Hu, S., et al., *Ni3N/NF as bifunctional catalysts for both hydrogen generation and urea decomposition.* ACS applied materials & interfaces, 2019. **11**(14): p. 13168-13175.

31. Babar, P., et al., *Bifunctional 2D electrocatalysts of transition metal hydroxide nanosheet arrays for water splitting and urea electrolysis.* ACS sustainable chemistry & engineering, 2019. **7**(11): p. 10035-10043.
32. Babar, P., et al., *Trifunctional layered electrodeposited nickel iron hydroxide electrocatalyst with enhanced performance towards the oxidation of water, urea and hydrazine.* Journal of colloid and interface science, 2019. **557**: p. 10-17.
33. Jia, X., et al., *Amorphous Ni(III)-based sulfides as bifunctional water and urea oxidation anode electrocatalysts for hydrogen generation from urea-containing water.* Applied Catalysis B: Environmental, 2022. **312**: p. 121389.